

# An analysis of the Performance and Economic Feasibility of a Hybrid Solar Cooling System that Combines an Ejector with Vapor Compression Cycles, Powered by a Photovoltaic Thermal (PV/T) Unit

Ghassan M. Tashtoush\*, Mohammad A. Alzoubi

Department of Mechanical Engineering, Jordan University of Science and Technology, Irbid, Jordan

Received 3 Sep 2022

Accepted 5 Jan 2023

## Abstract

Solar cooling technologies have become essential, especially in tropical countries due to the amount of solar radiation and the growing need for cooling. Gigantically, this study aims to depict a hybrid solar cooling system driven by a photovoltaic/thermal unit. The PV cells are used to power a Vapor Compression Refrigeration (VCR) cycle; whereas the waste thermal energy that has been utilized from cooling the PV modules is applicably used to run the Ejector Cooling Refrigeration (ECR) cycle. A mathematical model of the system has been generated to simulate this hybrid solar cooling system. The electrical energy derived from the PV cells was used to run the (VCR) cycle, resulting in a cooling capacity that ranges from a minimum of 3.215 kW to a maximum of 3.99 kW. Meanwhile, the heat utilized by cooling the PV modules was used to run the ECR resulting in an additional cooling capacity arranges from a minimum of 1.85 to a maximum of 2.46 kW. Consequently, as a result, the total cooling capacity of the hybrid system arranges from 5.14 kW to 6.4 kW with a COP of 5.8 and a maximum of 6.9 have been occupied during the period of study. Compared to the conventional VCR cycle powered by a solar non-cooled PV unit, the hybrid system has produced 24.8% increasingly more cooling capacity while using the same (25 m<sup>2</sup>) area of panels in July privately when running the system for 18 hours. Based on the economic viability of the system, crucially the payback period of the added cost from combining the VCR with the ECR systems will be returned within 7.3 years.

© 2023 Jordan Journal of Mechanical and Industrial Engineering. All rights reserved

**Keywords:** ECR, VCR, Combined Cooling Cycles, Solar Cooling, COP Enhancement.

## NOTATIONS & ABBREVIATIONS

NOTATIONS	
$P_{PV}$	Electrical power generated by PV cell (watt)
$I$	Solar radiation Intensity (W/m <sup>2</sup> )
$(\tau\alpha)_{PV}$	The product of effective absorptivity and transmissivity for the PV cells
$\eta_{PV}$	PV cell electrical efficiency
$\eta_{T,ref}$	PV cell electrical efficiency as the reference temperatures
$\beta_{ref}$	Cell efficiency temperature coefficient (K <sup>-1</sup> ) for the reference temperature
$T_{PV}$	The temperature of PV cell (K)
$T_{ref}$	PV cell efficiency reference temperature
$Q$	Energy Rate (watt)
$Q_{T,H,L}$	Thermal energy loss (watts)
$h_U$	Convection heat transfer coefficient $\frac{W}{m^2.K}$
$A_U$	Heat transfer area (m <sup>2</sup> )
$\Delta T_{LM}$	Log mean temperature difference (°C)
$C_p$	Specific heat of water at constant pressure (J/kg.K)
$C_v$	Specific heat of water at constant volume (J/kg.K)

$\dot{m}$	Mass flow rate (kg/s)
$p$	Pressure (Bar)
$T$	Temperature (K)
$A$	Area (m <sup>2</sup> )
$\gamma$	Specific Heat Ratio
$\eta_p$	Coefficient Related to the Isentropic Efficiency of the Primary Flow
$\eta_s$	Coefficient Related to the Isentropic Efficiency of the Secondary Flow
$R_{gas}$	General Gas Constant kJ/kg.K
$M$	Mach Number
$\phi_p$	Coefficient Related to the Primary Flow Losses
$\phi_m$	Coefficient Related to the Mixed Flow Losses
$V$	Velocity (m/s)
$a$	Speed of sound (m/s)
$r_e$	Expansion Ratio
$r_p$	Compression Ratio
$X$	Quality
$Q_c$	Condenser Rate of Heat Transfer (kW)
$Q_e$	Evaporator Rate of Heat Transfer (kW)
$h$	Enthalpy kJ/kg
$W_p$	Pumping Power (kW)

\* Corresponding author e-mail: gtash@just.edu.jo.

$W_c$	VCR compressor work (kW)
<b>ABBREVIATION</b>	
$EL$	Electrical
$TH$	Thermal
TH. L	Thermal Loses
u	Useful
AC	Air Conditioner
$i$	Inlet of the PV/T Panels
$c$	Condenser
$e$	Evaporator
$g$	Generator
$VCR$	Vapor Compression Refrigeration
$ECR$	Ejector Cooling Refrigeration
$t$	Throat
$p_l$	Primary nozzles exit plane
$m$	Mixed Flow inside the ejector
$p$	Primary Flow (from the generator to ejector)
$s$	Secondary Flow (from the evaporator to the ejector)
$p_y$	Primary Flow at the Entrained Flow Chocking Location
$s_y$	Secondary Flow at the Entrained Flow Chocking Location
1	Primary Nozzle Exit Plane
2	Constant Area Chamber Inlet Plane
3	Constant Area Chamber Exit Plane
$C_t$	Cash Flows (JOD)
N	The lifetime of the investment
I	Interest Rate
T	Time/Years
$Exp$	Experimental
$Theo$	Theoretical
$EES$	Engineering Equations Solver
$COP$	Coefficient of Performance
PBP	Pay Back Period (Year)

## 1. Introduction

Currently, global warming is getting more dangerous, electricity prices are increasing, and the air-conditioning applications demand is much higher than before, which made the researchers develop and investigate new types of air conditioning technologies or develop the existing ones, or even combine multi-systems. A way to reduce the electrical consumption globally was to investigate a new method to utilize the solar energy for cooling.

ALShqirate et. al [1] conducted an experimental and analytical study on the cooling of superheated carbon dioxide gas, focusing on the heat transfer and pressure drop in mini and microtubes. An experimental investigation along with an analytical study was carried out in this work. It was intended to be part of the supercritical Gustav Lorentzen refrigeration cycle of CO<sub>2</sub>.

Armand Noël et. al [2] have studied a VCR cooling cycle driven by a PV panel for dry and tropical regions, their results show that for an evaporating temperature of 0 °C, the effective power of the compressor varies between 5.33 kW and 6 kW, and the coefficient of performance varies from 3.28 to 3.74. What must be clarified; they have run a VCR cycle while using the electrical energy obtained from the PV panels, meanwhile; there is an enormous portion of waste solar energy that has not been utilized.

Photovoltaic efficiency is highly affected by its surface temperature. One degree increment for its surface could decrease its efficiency by about 0.45 - 0.5%, most of the solar energy captured by the PV is converted to thermal energy, and some to electrical energy which leads to worse PV efficiency, so, it was important to reduce these thermal

energies by cooling the PV and reuse the wasted heat, which increases the overall efficiency and the PV lifetime. [3-5].

### 1.1. Solar PV Panel Cooling System

Ben Cheikh et. al [6] attempted to study the thermal and electrical performance of solar PV panel cooling. They found that the natural circulation of air is the easiest and has a lower cost to remove heat from the panel, as result, PV/T efficiency is about 54.5% in the water-cooled and 16.24% in air-cooled. Maharane et. al [7] studied one of the crucial elements for mastering the performance of a Stand Alone PV System (SAPVS), which is the control and management of energy storage

A. N. Özakinet. al [8] took the benefit of the waste heat from the PV panel by air cooling, to increase the overall efficiency of the system, as a result, 0.1 °C increasing the cooling fluid provides the system with about 4.85W thermal power.

S. Odeh et. al [9] used a trickling cooling technique for the upper surface of the panel, and M. Zohri et. al [10] found that an integrated PV/T system with a V Grove collector has much better efficiency than the regular collectors, M. Abdolzadeh et. al [11] studied the effect of cooling the PV panel by spraying water on the panel surface, and Rosa-Clot et. al [12] studied the performance of submerged PV panels in water. There are several uses of thermal generating by the PV instead of rejecting them to the environment. L. Rekha et. al [13] used this thermal energy for heating domestic systems, also S. Zafar et. al [14] combined PV/T with a fuel cell to generate electricity, hydrogen, and water. PV/T could reach high thermal temperature, according to the connection of the PV panels, and the water tube configurations.

Badran et. al [15] used the fuzzy sets methodology to evaluate the most suitable solar technologies for power generation in Jordan, namely solar ponds and photovoltaic (PV) technologies.

Shyam et. al [16] presented a numerical model of PV/T panels series-connected which reached a temperature of 100 °C at the last panel outlet, PV/T panels can achieve high thermal temperatures, depending on the mass flow rate and the connection configuration ranges from 75-100 °C [17, 18]. Moh'd A. Al-Nimr et. al [19] proposed a system that takes advantage of the waste heat generated by the CPV/T to run an absorption system using LIBR-Water working fluid and TEC to produce electricity and cooling, the thermal waste from the CPV/T used in the VAR and the electricity in the TEC.

Nijmeh [20] conducted a technical and economic evaluation of the application of phase change material (PCM) in the cooling and thermal regulation of photovoltaic (PV) panels in Jordan. This technical study was performed based on experimental tests carried out on two identical 3.99 kWp PV systems for one full year at Hashemite University, Jordan.

B. Su et. al [21] to increase the production of mechanical power from the Kalina cycle, used the cooling from the absorption chiller to cool the turbine outlet fluid from the Kalina cycle. M. A. Al-Nimret. al [22] studied how possible is to combine PV for water distillation, they investigated the CPV/T to generate electricity and distilled



What might not be mistaken, the energy source for the combined system is solar energy, PV/T panels convert solar radiation into two types of energy, initially, the electrical energy from the PV cells which is relatively small in Photovoltaics technology, while the second is the waste thermal energy which is higher than the electrical energy and usually it is wasted, in this system, it been utilized from the PV cells, naturally; electricity will be stored in batteries to run a VCR cycle, and the thermal energy will be stored in a water tank to feed the ECR cycle, storage is mandatory to guarantee a steady cooling output when the solar radiation is insufficient such as at nights or on cloudy days.

The system was driven by a PV/T system, and solar radiation which is received by the panels is typically converted into two types of energy; direct electrical energy by the PV cells and thermal energy which was beneficiary utilized from the PV panel's waste heat, spectacularly the system will work for 18 hours, from May to October where these months require the space cooling.

Starting with the photovoltaics efficiency calculations, it is essentially important to find the amount of electricity that will be used to run the VCR cycle, depending on the PV model specification which was chosen for the study.

It is a fact that Solar radiation that has been collected by the panels was not converted by the PV cells into useful energy, and that the waste energy in the form of heat, and besides some of this waste energy will be collected and stored by the water in a tank to use it to run the ejector cooling cycle as well.

### 3. Modeling and Simulation

#### 3.1. PV/T Collector

Accurately to simplify the theoretical model analysis, the following assumptions were considered:

1. Steady-state conditions.
2. The layer thickness effect of PV glass is neglected.
3. The glass absorptivity is ignored.

To determine the useful amount of solar energy obtained from the PV/T as the following [36]:

$$Q_s = I * A_{PV} * (\tau\alpha)_{PV} \quad (1)$$

The temperature affects the electrical efficiency of the photovoltaic panel ( $\eta_{PV}$ ), as follows[37]:

$$\eta_{PV} = \eta_{T,ref} (1 - \beta_{ref}(T_{PV} - T_{ref})) \quad (2)$$

For a given radiation power  $Q_s$ , the electrical energy  $Q_{EL}$ , and the thermal energy  $Q_{TH}$ , as follows [38]:

$$Q_{EL} = (Q_s * \eta_{PV}) \quad (3)$$

The thermal power obtained by the receiver:

$$Q_{TH} = Q_s * (1 - \eta_{PV}) \quad (4)$$

The useful energy obtained by the system after the losses for the back surface of the panels, the front surface, and the ambient radiation is as follows:

$$Q_{TH,L} = U_L * A(T_{PV} - T_a) \quad (5)$$

$$Q_u = Q_{TH} - Q_{TH,L} \quad (6)$$

#### 3.2. Vapor Compression Cycle

The following assumptions have been taken into consideration:

1. The evaporator and Condenser are constant pressure devices ( $P_4=P_1$  &  $P_3=P_2$ ).
2. Saturated liquid at the condenser outlet.

3. Steady operating conditions.
4. Adiabatic expansion process.

##### 3.2.1. Condenser

The condenser removes the heat from the working fluid which changes the fluid's phase. The heat removed by the condenser can be calculated using:

$$Q_{cVCR} = \dot{m}(h_8 - h_7) \quad (7)$$

##### 3.2.2. Expansion Valve

The expansion valve is a device that is used to reduce the pressure of the high-pressure region to the pressure of the low-pressure. The expansion process is an adiabatic process which means the inlet and outlet enthalpy of this process are equal:

$$h_8 = h_9 \quad (8)$$

##### 3.2.3. Evaporator

The evaporator is a heat-absorbing device, which absorbs the heat from the required space by the working fluid. The rate of heat absorbed by the evaporator can be calculated using:

$$Q_{evcr} = \dot{m}(h_{10} - h_9) \quad (9)$$

##### 3.2.4. Compressor

The compression process takes place to raise the refrigerant pressure which also increases the temperature and by assuming the mechanical efficiency of the compressor is 100%. The work done by the compressor can be calculated by:

$$W_c = h_7 - h_{10} \quad (10)$$

The Coefficient of Performance (COP) is defined as the heat removed from the space divided by the work done to remove the heat by the compressor. The coefficient of performance of the cycle can be calculated as:

$$COP = \frac{Q_{e,vcrc}}{W_c} \quad (11)$$

#### 3.3. Cooling Ejector

To simplify the ejector cooling cycle theoretical model, there is an assumption as follows:

1. Steady flow.
2. One dimensional.
3. Ideal working fluid
4. Constant properties
5. Adiabatic inner wall for the ejector
6. Neglecting kinetic energy at the nozzle entrance.
7. The mixing pressure is the same for both fluids.
8. The isentropic relations are approximated to simplify the analysis.

The two streams start to mix at the cross-section y-y (hypothetical throat) with uniform pressure,  $P_{py} = P_{sy}$  before the shock which is at the cross-section s-s.

The model shown in figure 2 and presented in the study was based on a model introduced by Huang et al. [39] and validated to check the ability of the Huang's system design of the presented model. The primary flow gains heat due to its passing through a generator, then it passes through the primary nozzle. For a given inlet stagnant pressure  $P_g$  and temperature  $T_g$ , the mass flow through the nozzle at choking conditions follows the following gas dynamic equation and the generator temperature equals the PV/T temperature -10 °C [12]:

$$Q_{th} = m \cdot cp \cdot (T_i - T_o) \quad (12)$$

$$m_p^o = \frac{p_g A_t}{\sqrt{T_g}} \times \sqrt{\frac{\gamma}{R} \left(\frac{2}{\gamma+1}\right)^{\frac{\gamma+1}{\gamma-1}} \sqrt{\eta_p}} \quad (13)$$

The gas-dynamic relations between the Mach number at the exit of the nozzle  $M_{pl}$ , the exit cross-section area  $A_{pl}$  and pressure  $P_{pl}$  are using isentropic relations as an approximation:

$$\left(\frac{A_{p1}}{A_t}\right)^2 \approx \frac{1}{M_{p1}^2} \left[\frac{2}{\gamma+1} \left(1 + \frac{\gamma-1}{2} M_{p1}^2\right)\right]^{\frac{\gamma+1}{\gamma-1}} \quad (14)$$

$$\frac{p_g}{P_{p1}} \approx \left(1 + \frac{\gamma-1}{2} M_{p1}^2\right)^{\frac{\gamma}{\gamma-1}} \quad (15)$$

The primary flow from section 1-1 to section y-y where Mach number  $M_{py}$  of the primary flow at the y-y section follows the isentropic relations:

$$\frac{P_{py}}{P_{p1}} \approx \left(\frac{1 + \frac{\gamma-1}{2} M_{p1}^2}{1 + \frac{\gamma-1}{2} M_{py}^2}\right)^{\frac{\gamma}{\gamma-1}} \quad (16)$$

For the area calculations of the primary flow core at the y-y section, by using the following isentropic relation, including the coefficient  $\theta p$  to account for the loss of the primary flow from sections 1-1 to y-y:

$$\frac{A_{py}}{A_{p1}} = \frac{\frac{\theta p}{M_{py}} \left[\frac{2}{\gamma+1} \left(1 + \frac{\gamma-1}{2} M_{py}^2\right)\right]^{\frac{\gamma+1}{2(\gamma-1)}}}{\frac{1}{M_{p1}} \left[\frac{2}{\gamma+1} \left(1 + \frac{\gamma-1}{2} M_{p1}^2\right)\right]^{\frac{\gamma+1}{2(\gamma-1)}}} \quad (17)$$

The loss may result from the slipping or viscous effect of the primary and the entrained flows at the boundary. For a given inlet stagnant pressure  $P_e$ , the following equation is applied:

$$\frac{P_e}{P_{sy}} \approx \left(1 + \frac{\gamma-1}{2} M_{sy}^2\right)^{\frac{\gamma}{\gamma-1}} \quad (18)$$

The secondary (entrained) flow rate at choking condition could be determined as this equation:

$$m_s = \frac{P_e \times A_{sy}}{\sqrt{T_e}} \times \sqrt{\frac{\gamma}{R} \left(\frac{2}{\gamma+1}\right)^{\frac{\gamma+1}{\gamma-1}} \sqrt{\eta_s}} \quad (19)$$

The geometrical cross-sectional area at sections y-y is  $A_3$  that is the sum of the areas for the primary flow  $A_{py}$  and the entrained flow  $A_{sy}$ .

$$A_3 = A_{py} + A_{sy} \quad (20)$$

The temperature and the Mach number of the two streams at sections y-y follows:

$$\frac{T_g}{T_{py}} = 1 + \frac{\gamma-1}{2} M_{py}^2 \quad (21)$$

$$\frac{T_e}{T_{sy}} = 1 + \frac{\gamma-1}{2} M_{sy}^2 \quad (22)$$

A momentum balance relation thus can be derived as:

$$\theta_m [\dot{m}_p \times V_{py} + \dot{m}_s \times V_{sy}] = (\dot{m}_p + \dot{m}_s) V_m \quad (23)$$

An energy balance relation can be derived as

$$\dot{m}_p \left(C_p T_{py} + \frac{V_{py}^2}{2}\right) + \dot{m}_s \left(C_p T_{sy} + \frac{V_{sy}^2}{2}\right) = (\dot{m}_p + \dot{m}_s) \left(C_p T_m + \frac{V_m^2}{2}\right) \quad (24)$$

Where  $V_{py}$  and  $V_{sy}$  are the gas velocities of the primary and entrained flow at section y-y:

$$V_{py} = M_{py} \times a_{py}; \quad a_{py} = \sqrt{\gamma R T_{py}} \quad (25)$$

$$V_{sy} = M_{sy} \times a_{sy}; \quad a_{sy} = \sqrt{\gamma R T_{sy}} \quad (26)$$

The Mach number of the mixed flow can be evaluated using the following relation:

$$M_m = \frac{V_m}{a_m}; \quad a_m = \sqrt{\gamma R T_m} \quad (27)$$

The following gas dynamic relations exist:

$$\frac{P_3}{P_m} = 1 + \frac{2\gamma}{\gamma+1} (M_m^2 - 1) \quad (28)$$

$$M_3^2 = \frac{1 + \frac{\gamma-1}{2} M_m^2}{\gamma M_m^2 - \frac{\gamma-1}{2}} \quad (29)$$

The pressure at the exit of the diffuser follows the relation, assuming an isentropic process:

$$\frac{P_c}{P_3} = \left(1 + \frac{\gamma-1}{2} M_3^2\right)^{\frac{\gamma}{\gamma-1}} \quad (30)$$

According to the above model simulation, the performance of the ejector can be investigated as:

$$\omega = \frac{\dot{m}_s}{\dot{m}_p} = \frac{P_e A_{sy}}{P_g A_t} \sqrt{\frac{T_g \eta_s}{T_e \eta_p}} \quad (31)$$

Substantially it sounds crucial also to debate the following parameters:

$$r_e = \frac{P_g}{P_e} \quad (32)$$

$$r_p = \frac{P_c}{P_e} \quad (33)$$

The expansion ratio ( $r_e$ ) which represents the ratio of the primary flow pressure to the secondary flow pressure and the compression ratio ( $r_p$ ) which is the condenser pressure to the evaporator pressure.

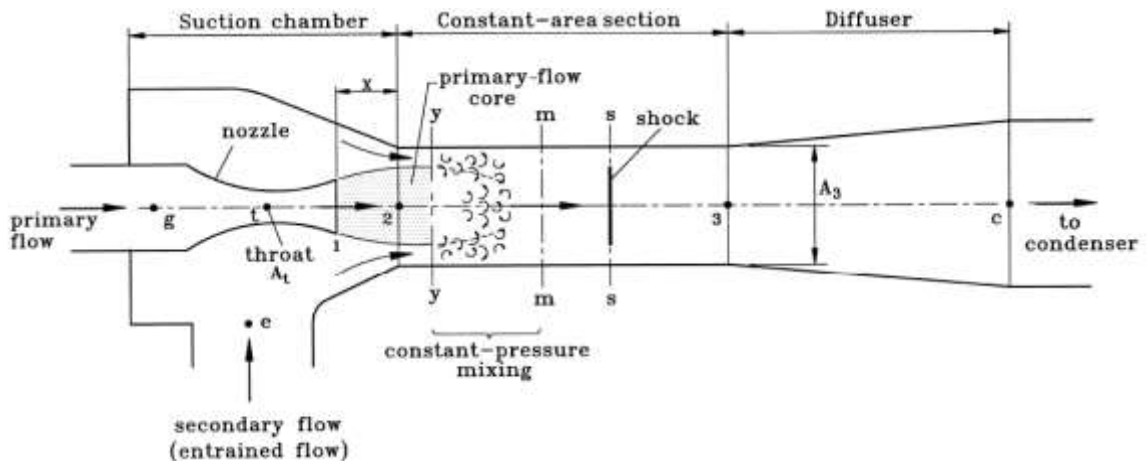


Figure 2. Schematic Diagram of the ejector performance [39].

### 3.3.1. Generator

To calculate the energy rate consumed by the generator the first law of thermodynamics was applied as follows:

$$\dot{Q}_g = \dot{m}_p(h_2 - h_1) \quad (34)$$

as:

$$h_2 = h(T = T_g, x = 1), h_1 = h(T = T_c, P = P_c)$$

### 3.3.2. Condenser

To calculate the energy rate rejected by the condenser the first law of thermodynamics was applied as follows:

$$\dot{Q}_{CECR} = (\dot{m}_p + \dot{m}_s)(h_5 - h_4) \quad (35)$$

$$\dot{m}_p h_2 + \dot{m}_s h_3 = (\dot{m}_p + \dot{m}_s) h_4 \quad (36)$$

as:

$$h_5 = h(T = T_c, x = 1)$$

### 3.3.3. Throttling Valve

The throttling process is assumed to be an adiabatic process, which means the enthalpy at the valve inlet and outlet are the same.

$$h_5 = h_6 \quad (37)$$

### 3.3.4. Evaporator

The first law of thermodynamics was applied as follows to find the cooling capacity of the evaporator.

$$\dot{Q}_{eECR} = \dot{m}_s(h_3 - h_6) \quad (38)$$

$$h_3 = h(T = T_e, x = 1)$$

### 3.3.5. Mechanical Pump

The pumping power required to deliver the liquefied refrigerant from the condenser to the generator can be evaluated by:

$$\dot{W}_{pump} = \dot{m}_p \frac{P_g - P_c}{\rho} \quad (39)$$

$$\rho = \rho(T = T_c, P = P_g)$$

Ejector Cooling Cycle Performance

The coefficient of performance can be given by:

$$COP = \frac{\dot{Q}_{eECR}}{\dot{Q}_g} = \omega \frac{h_3 - h_6}{h_2 - h_1} \quad (40)$$

## 3.4. System Performance

Evaluating the system's performance is equal to the total cooling load achieved by the system divided by the electricity consumed by the VCR compressor and the system's pumps, thermal energy utilized from the PV/T was not considered as energy input to the system; logically, while it is a waste.

$$COP_{sys} = \frac{1}{Q_{eVCR} + Q_{eECR}} \quad (41)$$

## 4. Simulation Input Parameters

Input parameters are presented in Tables 1, 2, and 3. Representative ejector cooling cycle inputs were chosen according to the recommendations of the literature as demonstrated [39].

### 4.1. System Validation

#### 4.1.1. Ejector Results Validation

The ejector cooling model has been compared with the theoretical and experimental results which are provided by Huang [39]; the comparison is shown in table 4.

Subsequently, the current model results have depicted a prospective agreement with Huang's [39] experimental results. a sample of three ejectors studied by Huang [39] has validated the current model, however; Huang's models are named (AA, AB, and AC). Table 4 points out the presented work results and Huang's theoretical and experimental results and the error of the presented model and Huang's theoretical models.

There is a visible grasp, the error of the entrainment ratio was calculated compared to the experimental results which are provided by Huang [39] as follows:

$$\% \text{ error} = \frac{|\omega_{Exp} - \omega_{Theo}|}{\omega_{Exp}} \quad (42)$$

**Table 1.** PVT input parameter

Parameter	Value
Panels Area(A)	25 m <sup>2</sup>
Cell efficiency temperature coefficient ( $\beta$ )	0.004
Cell reference Temperature ( $T_{ref}$ )	25°C
Reference Efficiency ( $\eta_o$ )	0.14
Transmissivity ( $\tau_{pv}$ )	0.92
Absorptivity ( $\alpha_{pv}$ )	0.9

**Table 2:** Cooling Ejector input parameters

Parameter	Value
Working Fluid	R134a
Throat Diameter (dt)	0.000508 m
Specific heat Ratio ( $\gamma_{R134a}$ )	1.2
Area Ratio (A3/At)	4.86
Isentropic efficiency of the primary flow ( $\eta_p$ )	0.95
Isentropic efficiency of the secondary flow ( $\eta_s$ )	0.85
The Frictional Loses coefficient of the primary flow ( $\phi_p$ )	0.88
The Frictional Loses coefficient of the mixed flow ( $\phi_m$ )	0.84
Evaporator Temperature	5 °C
Condenser Temperature	Ambient Temperature +5 °C

**Table 3:** Vapor Compression Cycle input parameters

Parameter	Value
Evaporator Temperature	5 °C
Condenser Temperature	Ambient Temperature +5 °C
Isentropic efficiency of the compressor	0.6
Working Fluid	R134a

**Table 4.** Comparing the present model of the ejector with the theoretical and experimental results provided by Huang [39].

Ejector	Area Ratio	Primary Flow		Secondary Flow		Presented Work	Theoretical by Huang [39]	Experimental by Huang [39]	Presented work error	Huang[39] error
		T (K)	P (bar)	T (K)	P (bar)					
AA	6.44	368	6.04	281	0.04	0.1785	0.1554	0.1859	4%	16.4%
		363	5.38			0.2241	0.2156	0.2246	0.2%	4.0%
		357	4.65			0.29	0.288	0.288	1%	0.0%
		351	4			0.3677	0.3525	0.3257	13%	8.2%
		368	6.04	285	0.047	0.2468	0.2573	0.235	5%	9.5%
		363	5.38			0.3011	0.3257	0.2946	2%	10.6%
		357	4.65			0.3793	0.4147	0.3398	12%	22.0%
AB	6.99	363	5.38	281	0.04	0.2679	0.2093	0.2718	1%	23.0%
		357	4.65			0.3402	0.3042	0.3117	9%	2.4%
		351	4			0.4255	0.4422	0.3922	8%	12.7%
AC	7.73	368	6.04	281	0.047	0.2705	0.2983	0.2814	4%	6.0%
		363	5.38			0.3268	0.3552	0.3488	6%	1.8%
		357	4.65			0.4079	0.4605	0.4241	4%	8.6%
		351	4			0.5033	0.5966	0.4889	3%	22.0%
Avg. Error									5%	10.51%

**4.1.2. Solar System Results Validation**

Solar system simulation was validated by **Swapnil Dubey et. al [40]**, they analyzed and studied a PV/T flat plate water collector connected in series, the parameter to validate the current model with, was electrical efficacy, comparing the results for the hourly variation of electrical efficiency concerning panels quantity. The following table 5 shows the presented work model results with Swapnil’s results.

**4.1.3. VCR System Validation Results**

The VCR cycle simulation in the presented study was validated by Mehmet Bilgili [41], he has done an hourly simulation and performance of solar electrically powered VCR cycle, a validation for the cycle COP of the presented work model and Mehmet Bilgili’s work is presented in table 6 below.

**5. Results and Discussion**

**5.1. 5.1 PV/T**

It is plain that solar radiation is the proposed system’s energy source. The energy from the solar radiation was converted into two types of energy; initially, electrical energy from the PV to run the VCR cycle, and secondly, thermal energy by utilizing the waste heat from the PV cells to run the cooling ejector. The solar radiation for the Jordan Northern was the presented system’s energy input, as average monthly solar radiation. The system is used mainly for cooling purposes, which means the study is involved in the months from May-October. Hereby on focusing, Figure 3 below depicts the measured monthly average solar radiation per square meter using a local weather station for the analyzed location in the city of Irbid

(The latitude of Irbid, Jordan is 32.551445, and the longitude is **35.851479**). This has resulted in the electrical energy being obtained as figure 4 shows and the thermal energy as figure 5 shows.

**Table 5.** Comparing the electrical efficiency for the presented work model of the solar system with the theoretical results provided by Swapnil Dubey[40].

Time of the day	Presented Work	Swapnil Dubey [40]	Error
9 AM	0.99	0.98	1.02 %
10	0.961	0.945	1.69 %
11	0.912	0.89	2.47 %
12	0.87	0.86	1.16 %
13	0.868	0.865	0.35 %
14	0.86	0.87	1.15 %
15	0.912	0.92	0.87 %
16	0.954	0.97	1.65 %

**Table 6:** Comparing the Cycle’s COP for the presented work model of the VCR cycle with the theoretical results provided by Mehmet Bilgili[41].

Time of the day	Presented Work (COP)	Mehmet Bilgili [41] (COP)	Error
8 AM	5.4	5.51	2.00 %
9	5.09	5.2	2.12 %
10	4.76	4.9	2.86 %
11	4.5	4.6	2.17 %
12	4.45	4.52	1.55 %
13	4.23	4.4	3.86 %
14	4.36	4.38	0.46 %
15	4.45	4.37	1.83 %
16	4.52	4.39	2.96 %
17	4.51	4.41	2.27 %

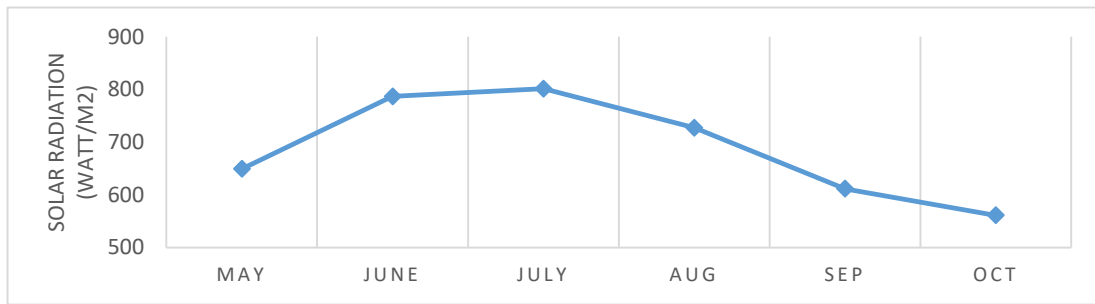


Figure 3. Monthly average solar radiation for the proposed system's location.

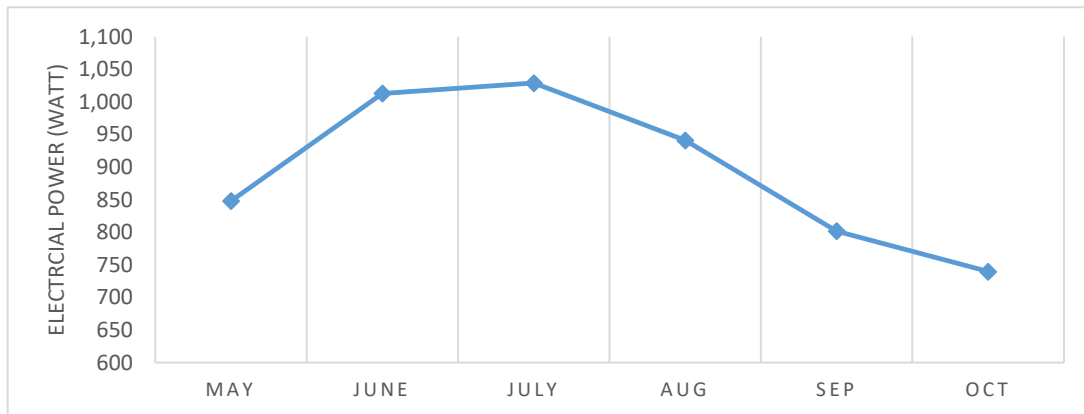


Figure 4. Achieved electrical power from the PV/T for the proposed system's location.

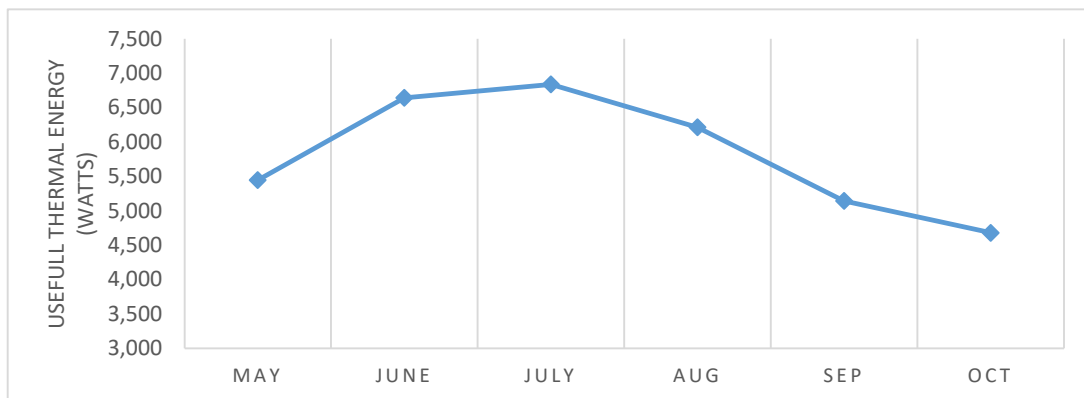


Figure 5. Useful thermal energy obtained from the PV/T for the proposed system's location.

### 5.2. Vapor Compression Cycle

Historically in concern, the cooling capacity also depends on the evaporator temperature and the solar radiation as figure 6 explores, increasing the evaporator temperature which increases the pressure of the low-pressure region for the VCR cycle which makes the compressor consumes goes less energy than the lower evaporator temperatures, and, what seems flashy while, the cycle input power remains the same, the mass flow rate of the refrigerant in the cycle will rise to consume all the input energy, which led to a higher cooling capacity for the cycle and as having discussed in figure 6 previously, the effect of ambient temperature has provided less COP to the cycle in July and August, but respectively in July the cycle provided more cooling capacity, which seems to be the highest solar radiation obtained in July which was converted into a higher amount of electrical energy to feed the cycle.

The vapor compression cycle is the most used type of refrigeration cycle for the cooling or refrigeration purposes. Figure 7 explains the variation of the VCR cycle COP with the monthly average solar radiation and the evaporator temperature, keeping into consideration that the evaporator temperatures were assumed to react in resembling same as the ejector's evaporator temperatures, however; the evaporators for both cooling cycles are historically sharing the same indoor unit but with separated pipes. As shown in figure 7, in July the COP decreased from 3.5 to 2.9 respectively in comparison to May, meanwhile; July has more phenomenal solar radiation than May, if I might not be mistaken, the reason for that is due to the condenser temperature effect on the VCR cycle performance, nevertheless; the ambient temperature in July seems to be more gigantic than May which has grown up the condenser temperature, where significantly has impacted the cycle's COP. Furthermore, incitement about the evaporator temperature effect cooling cycles, by increasing the evaporator temperature what should be

focused on, its pressure will be increased, thus consequently; the compressor will consume less work to reach the desired pressure -condenser pressure- while keeping the cooling capacity constant.

5.3. Cooling Ejector

What stands out; a cooling ejector is counted to be a thermally driven cooling cycle mainly having used with a low-grade energy source. Evaporator temperature and average monthly solar radiation impact the ejector cooling capacity, besides the COP, apparently; the effect on cooling capacity has different manner than the COP effect, as figure 8 implicit, for July which has the highest solar radiation among the annual year, the ejector has achieved the highest amount of cooling capacity, it is in causality

because of the PV/T panels that having provided higher thermal energy, which has increased the kinetic energy for the primary flow in the generator used to feed the cooling ejector, which means in dictum; a reverse relationship between the average solar radiation and the cooling capacity crucially having been compared to COP as shown in figure 9.

What emerges massively is that the evaporator temperature occupies the same effect for both cooling capacity and COP, swanking the evaporator temperature will increase the pressure difference between the primary flow nozzle inlet and the entrained flow inlet, hence in this way; the primary form will entrain higher amount of the entrained (secondary) flow that increases the refrigerant mass flow rate in the ejector.

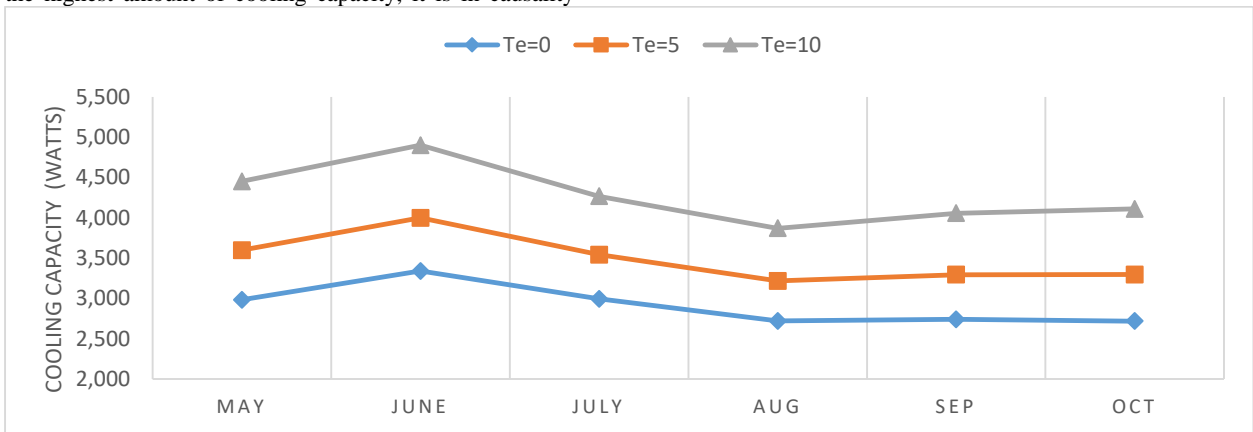


Figure 6. VCR cooling capacities for different evaporator temperatures and the average monthly solar radiation.

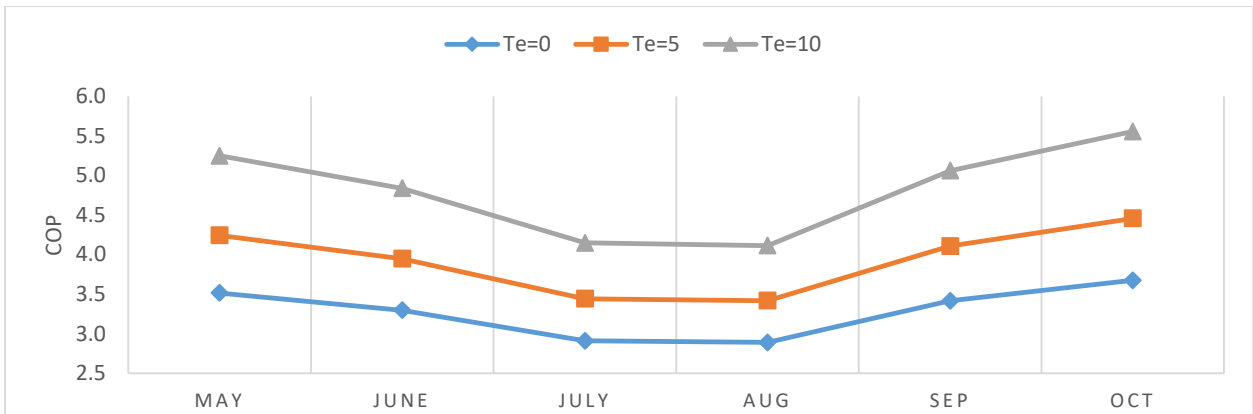


Figure 7. VCR cooling cycle COP for different evaporator temperatures and the average monthly solar radiation.



Figure 8. ECR cycle cooling capacity for different evaporator temperatures and the average monthly solar radiation.

Undoubtedly, it might seem murky, but the relationship between both the average monthly solar radiation and the evaporator temperature of the ejector as well as their effect on COP is crystalline shown in figure 9. What should be concluded; the solar radiation absorbed by the PV which is converted into thermal energy by cooling the PV panels is the ejector energy source, the ECR cycle COP has primarily a reverse relationship between the solar radiation and COP, hence; July has the highest solar radiation among the year for the proposed system location, meanwhile; it has the lowest COP. What should be genetical, the reason for having the lowest COP in the highest solar radiation month is counted to be because of two fundamental reasons, while the ejector COP is affected by the entertainment ratio, and by enlarging the generator temperature which occurs in the highest solar radiation months, the COP tends to increase, but respectively the increment of the entertainment ratio was too low to affect the COP significantly less than 1% as figure 10 below show. What could be summed up, the effect came from the high increment of solar radiation in July which differentiated from the increment of the cooling capacity (both have increased, but solar radiation increased with a higher ratio), which indicated to the COP decreases in July.

Beyond; what must be deemed, the evaporator temperature has also a relatively high impact on the ejector's COP, whereas decreasing the evaporator temperature leads to a decrease in the COP, situationally the reason for that is the ejector's COP is equal to the energy out (cooling capacity) to the energy in (thermal energy from the PV/T) thus correspondingly, decreasing the evaporator temperature will potentially decrease the kinetic energy of the entrained flow, and hence as a result, the efficiency of the suction process in the ejector decreases which directly will give less cooling capacity

than having obtained from the ejector. Usually as frequent, the most suitable evaporator temperature ranges from 5-8 °C for cooling applications.

Entrainment ratio is counted to be the ratio between the secondary to the primary refrigerant mass flow rates in the ejector, clearly figure 10 shows the variation of the ejector cycle entrainment ratio with the average monthly solar radiation, in July the ejector has the highest entrainment ratio that being compared to the other months, while entrainment ratio is affected by the generator temperature, and in July the system achieved the highest fluid output temperature led to a higher pressure difference in the ejector nozzle, which emits more secondary flow to the ejector increases then the entrainment ratio has already increased.

#### 5.4. System Performance

What seems visible; is the Entrainment ratio variation with the evaporator temperature and average monthly solar radiation presented in figure 11, it should be mentioned that when the evaporator temperature increases from 0 to 10 °C in May, for example, the entrainment ratio increases from 0.36 to 0.61. In other words, it increased by 69% because increasing the evaporator temperature enlarges the pressure difference between the entrained flow and primary flow regions, which provided the primary flow with the ability to entrain more refrigerant to the ejector. While on the other hand, with high thermal energy provided by the PV/T, the entertainment ratio has only increased by less than 1%, which means the evaporator temperature has a significantly and more impact on the ejector entrainment ratio than the solar radiation which affects the COP and cooling capacity significantly in comparison.

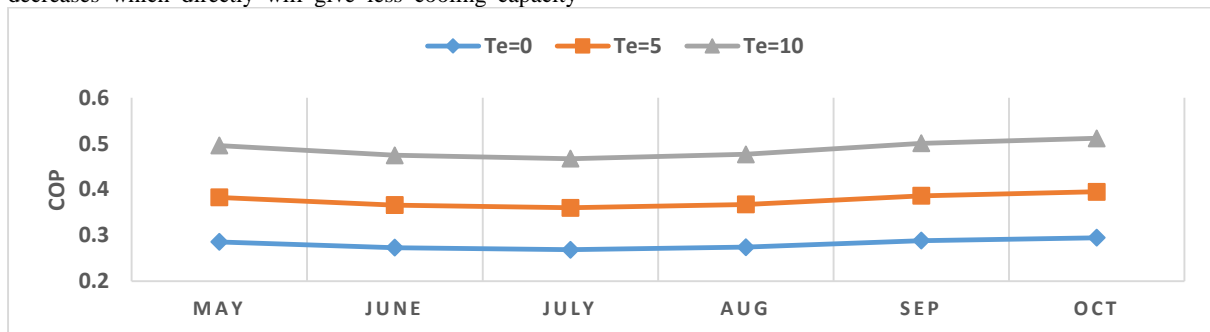


Figure 9. ECR cycle COP for different evaporator temperatures and the average monthly solar radiation.

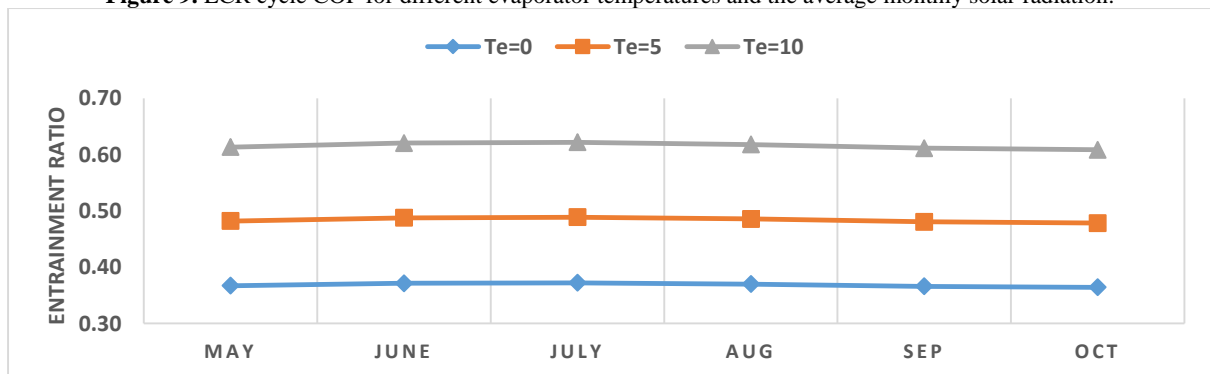


Figure 10. ECR cycle entrainment ratio for different evaporator temperatures and the average monthly solar radiation.

It is crystal clear that while assuming a system that is applied to the same area of PV panels that was exactly used in the proposed system; however, the power output from the panels will run a VCR cycle with a cooling capacity arranged from a minimum of 3,007 to maximum of 3,780 watts among the studied period, clearly as to how figure 11 denotes; meanwhile, the proposed system VCR cycle has obtained between 3,215 to 3,999 watt of cooling capacity with an average increment of 6.38% from cooling the PV, what never goes without citing according to [3-5] the efficiency of the PV has been significantly affected by the PV temperature.

To be obvious, COP for a cooling system seems to be equal to the cooling capacity, which is divided by the electrical energy, in the case being used to run the cycle; likewise, the electrical energy which has derived from the PV panels still reminds the same, in contrast; the cooling capacity has been tremendously enlarged because of running the ECR cycle. Consequently, the total system

coefficient of performance as figure 12 depicts. It has increasingly fluctuated by almost 40%, which indicates that it has grown up from the ratio of 3.2 to 5.8 in July.

It is distinctly clear, that Figure 13 illustrates a comparison between the proposed hybrid system components cooling capacities, the proposed system cooling capacity from the VCR was ranging minimum to maximum from 3,215 to 3,999 watts from May to October, and the ejector cooling cycle had a cooling capacity arranges from 1,848 to 2,462 watt, which was added to the system, and thence; keeping into consideration the effect of cooling the PV modules which increased the VCR cooling capacity as discussed in figure 6, the total cooling capacity of the system now arranges from 5,144 to 6,430 watt as a minimum and maximum among the cooling season respectively, which is 24.8% enhancement in July while being compared to a VCR driven by the PV panels only.

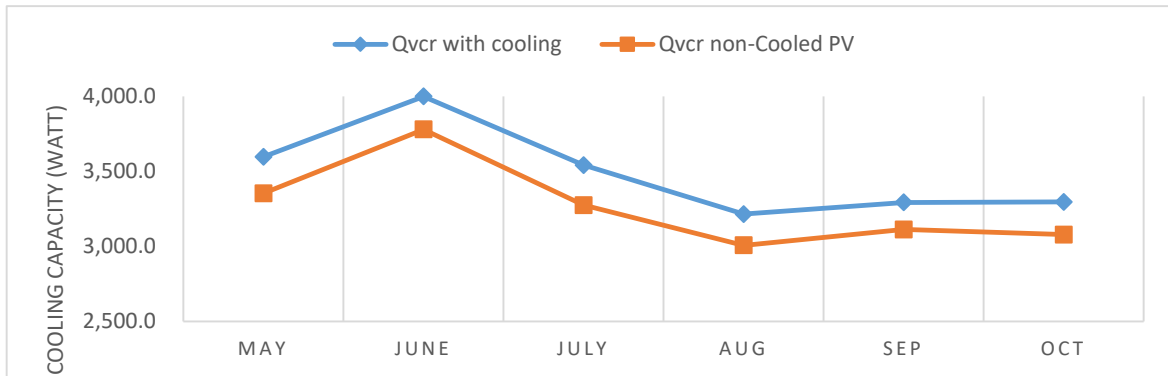


Figure 11. VCR cooling capacity comparison between the proposed hybrid system and a VCR cycle using PV only (for the same area of PV).

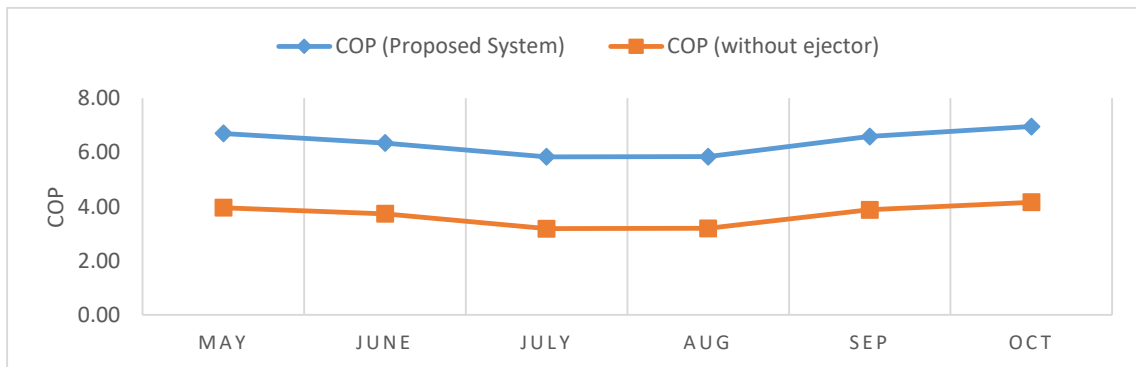


Figure 12. The proposed system total COP compared to the VCR cycle driven by PV-only variation and the average monthly solar radiation.

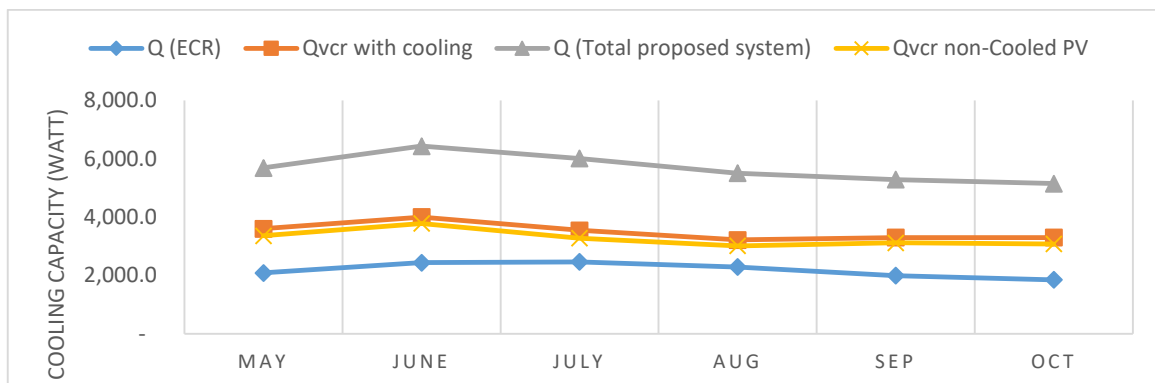


Figure 13: The proposed system component's cooling capacity.

## 6. Economic Analysis

What should be designated, following, Table 7 shows the cost of each component added to the system compared to the available systems.

**Table 7.** The presented model components cost [42].

Item	Local market cost (JOD)
Condenser	108
Evaporator	87
Refrigerant	114
Ejector	337
Pumps	148
Expansion valve	43
generator	199
Controller	371
piping network and fittings	219
installation cost	401
Maintenance cost	79
Water tank	78
Batteries (25 years)	776
<b>Total (JOD)</b>	<b>2,961</b>

The economic analysis was made for the extra components added to a single VCR cycle running using PV panels only, the ejector and components related to it to complete the proposed system were calculated, and the economic analysis was studied according to the extra cooling capacity obtained compared to a regular VCR system driven by PV panels.

For comparison purposes, the added components (ECR, Tank, Batteries, installation, and piping cost) were considered with the extra cooling capacity achieved. In this analysis, the electricity tariff, interest rate, and inflation rate are taken as 0.156 JOD/kWh, 5%, and 3%, respectively. 1% of inflation in the electricity tariff is considered. The maintenance and operation costs are considered as 2% of the capital cost annually, system's lifetime is 25 years.

The system is assumed to work (18 hours a day). The NPV method is used to evaluate the economic benefit of the proposed system. The definition of NPV is, [31, 38]

$$NPV = C_i + \sum_{t=1}^N \frac{C_t}{(1+i)^t} \quad (43)$$

$$C_t = C_{in} - C_{to} \quad (44)$$

And the PBP is calculated as:

$$C_t = \sum_{t=1}^{N_{PBP}} \frac{C_t}{(1+i)^t} \quad (45)$$

The power consumption of a conventional air condition unit of three stars rated equipment with an Energy Efficiency Ratio (EER) of 2.7 has been calculated as follows:

$$P = \frac{\text{Cooling Capacity (kW)}}{EER} \quad (46)$$

If would be saying, for the added 2.4 kW cooling capacity, the power consumption is 0.89 kWh. Meanwhile, the total electricity that is saved while using the proposed hybrid system is 2,435 kWh, while as; the system is 18 hours a day operating.

## 7. Conclusion

A Hybrid Vapor Compression / Ejector cooling system driven by a PV/T was introduced. The proposed system has utilized both thermal and electrical energies obtained from solar radiation and uses the PV/T collectors to run the two cooling cycles, VCR and ECR. The VCR was powered by the electrical power generated from the PV panels whereas the ECR cooling system was running by utilizing the wasted thermal energy obtained from cooling the panels. The results of this study can be summarized as follows.

1. When using a VCR operated by a PV panel without any cooling system, the VCR cycle provided a cooling effect arranged from 3,007-3,780 watts (minimum and maximum) during the period of study.
2. When the PV modules used to run the VCR cycle (proposed system) were cooled by a water-cooling system, the cooling capacity of the VCR increased from 3,215 to 3,999 watts.
3. The proposed system combined the ECR cycle with the regular VCR cycle. The ECR cycle operated by utilizing the waste thermal energy from cooling the modules provided a cooling effect ranging from 1,848 to 2,462 watts, this increased the total cooling capacity for the proposed hybrid system from 5,144.5 to 6,400.3 watts with a system total COP arranged from 5.8 to 6.9 as a minimum and maximum during the period of study.
4. While the area is not always available, which restricted the surface area for installing the PV panels to provide electricity to run the VCR cycle that is required for cooling an application. The presented hybrid system has gained an extra cooling capacity for the same PV surface area.
5. The proposed hybrid system could be used when high cooling capacity applications are needed with less surface area available for installing the PV system.
6. Based on the economic viability of the system, crucially the payback period of the added cost from combining the VCR with the ECR systems will be returned within 7.3 years.
7. The system assumed a 25 m<sup>2</sup> of panel area as a case study, bigger areas will act in the same manner, while the panel's area is bigger, the hot water obtained is more, same for electricity.

## References

- [1] ALShqirate, A., Hammad, M., & Tarawneh, M. (2012). Cooling of superheated refrigerants flowing inside mini and microtubes: Study of heat transfer and pressure drop, CO<sub>2</sub> case study. *Jordan Journal of Mechanical and Industrial Engineering*, 6(2), 199-203. ISSN 1995-6665.
- [2] Armand Noël Ngueche Chedop, Noël (2014) Djongyang, Zaatri Abdelouahab, Modelling of the Performance of a Solar Electric Vapor Compression Refrigeration System in Dry Tropical Regions. *International Journal of Science and Research (IJSR)*,3(11):1066-1076.
- [3] Dubey, S., Sarvaiya, J. N., & Seshadri, B. (2013). Temperature-dependent photovoltaic (PV) efficiency and its effect on PV production in the world - A review. *Energy Procedia*, 33, 311-321.

- [4] Reddy, S. R., Ebadian, M. A., & Lin, C. X. (2015). A review of PV-T systems: Thermal management and efficiency with single phase cooling. *International Journal of Heat and Mass Transfer*, 91, 861-871.
- [5] Skoplaki, E., & Palyvos, J. A. (2009). On the temperature dependence of photovoltaic module electrical performance: A review of efficiency/power correlations. *Solar Energy*, 83(5), 614-624.
- [6] H. Ben cheikh el hocine, K. Touafek, F. Kerrour, H. Haloui, A. Khelifa (2015) Model Validation of an Empirical Photovoltaic Thermal (PV/T) Collector, *Energy Procedia*, Volume 74, Pages 1090-1099, ISSN 1876-6102, <https://doi.org/10.1016/j.egypro.2015.07.749>.
- [7] Mahrane, A., Chikh, M., & Chikouche, A. (2010). Energy management for stand-alone PV system. *Jordan Journal of Mechanical and Industrial Engineering*, 4(1), 117-120. ISSN 1995-6665.
- [8] Özakin, A. N., Karsli, S., Kaya, F., & Güllüce, H. (n.d.). (2016) The heat recovery with heat transfer methods from solar photovoltaic systems. *Journal of Physics: Conference Series*, 707(1), 012050. <https://doi.org/10.1088/1742-6596/707/1/012050>
- [9] Odeh, S., & Behnia, M. (2009). Improving photovoltaic module efficiency using water cooling. *Heat Transfer Engineering*, 30(6), 499-505.
- [10] Zohri, M., Fudholi, A., Ruslan, M. H., & Sopian, K. (2017). Mathematical modeling of photovoltaic thermal PV/T system with the v-groove collector. *AIP Conference Proceedings*, 1862.
- [11] Abdolzadeh, M., & Ameri, M. (2009). Improving the effectiveness of a photovoltaic water pumping system by spraying water over the front of photovoltaic cells. *Renewable Energy*, 34(1), 91-96.
- [12] Rosa-Clot, M., Rosa-Clot, P., Tina, G. M., & Scandura, P. F. (2010). Submerged photovoltaic solar panel: SP2. *Renewable Energy*, 35(8), 1862-1865.
- [13] Rekha, L., Vijayalakshmi, M. M., & Natarajan, E. (2016). Photovoltaic thermal hybrid solar system for residential applications. *Energy Sources, Part A: Recovery, Utilization, and Environmental Effects*, 38(7), 951-959.
- [14] Zafar, S., & Dincer, I. (2014). Thermodynamic analysis of a combined PV/T-fuel cell system for power, heat, fresh water and hydrogen production. *International Journal of Hydrogen Energy*, 39(19), 9962-9972.
- [15] Badran, O., Abdulhadib, E., & Mamlook, R. (2010). Evaluation of solar electric power technologies in Jordan. *Jordan Journal of Mechanical and Industrial Engineering*, 4(1), 121-128. doi: 1995-6665
- [16] Tiwari, G. N., & Al-Helal, I. M. (2015). Analytical expression of temperature dependent electrical efficiency of N-PVT water collectors connected in series. *Solar Energy*, 114, 61-76.
- [17] Liang, R., Zhou, C., Pan, Q., & Zhang, J. (2017). Performance evaluation of sheet-and-tube hybrid photovoltaic/thermal (PVT) collectors connected in series. *Applied Thermal Engineering*, 122, 215-224.
- [18] Alobaid, M., Hughes, B., O'Connor, D., Calautit, J., & Heyes, A. (2018). Improving Thermal and Electrical Efficiency in Photovoltaic Thermal Systems for Sustainable Cooling System Integration. *Sustainability*, 10(2), 305-322.
- [19] Al-Nimr, M. A., & Mugdadi, B. (n.d.). (2020) A hybrid absorption/thermo-electric cooling system driven by a concentrated photovoltaic/thermal unit. *Energy*, 150, 439-450.
- [20] Nijmeh, S., Hammad, B., Al-Abed, M., & Bani-Khalid, R. (2020). A technical and economic study of a photovoltaic-phase change material (PV-PCM) system in Jordan. *Jordan Journal of Mechanical and Industrial Engineering*, 14(4), 371-379. ISSN 1995-6665.
- [21] Su, B., Jin, H., Hong, H., Qu, W., & Tang, S. (2018). A concentrating photovoltaic/Kalina cycle coupled with an absorption chiller. *Applied Energy*, 224, 481-493.
- [22] Al-Nimr, M. A., & Dahdolan, M. E. (2015). Modeling of a novel concentrated PV/T distillation system enhanced with a porous evaporator and an internal condenser. *Solar Energy*, 120, 593-602.
- [23] Al-Nimr, M. A., Al-Ammari, W. A., & Alkhalidi, A. (2019). A novel hybrid photovoltaics/thermoelectric cooler distillation system. *International Journal of Energy Research*, 43(2), 791-805.
- [24] Hamdan, M., Shehadeh, M., Al Aboushib, A., Hamdan, A., & Abdelhafez, E. (2018). Photovoltaic cooling using phase change material. *Jordan Journal of Mechanical and Industrial Engineering*, 12(3), 167-170.
- [25] Yılmaz, A., & Aktas, A. E. (2019). Comparative analysis of ejector refrigeration system powered with engine exhaust heat using R134a and R245fa. *Engineering, Mathematics and Science*, 3(1), 13-17.
- [26] Donga, J., Yua, M., Wang, W., Songa, H., Lia, C., & Pana, X. (2017). Experimental investigation on low-temperature thermal energy driven steam ejector. *International Journal of Heat and Mass Transfer*, 116, 716-724.
- [27] Selvaraju, A., & Mani, A. (2006). Experimental investigation on R134a vapor ejector refrigeration system. *International Journal of Refrigeration*, 29(4), 611-620.
- [28] Khalil, A., Fatouh, M., & Elgendy, E. (2011). Ejector design and theoretical study of R134a ejector refrigeration cycle. *International Journal of Refrigeration*, 34(7), 1684-1698.
- [29] Tolu, M. E., & Özen, D. N. (2018). Thermodynamic analysis of an ejector cooling system using R123 as refrigerant under different working conditions. *International Journal of Energy and Environmental Engineering*, 11(3), 281-289.
- [30] Varga, S., Oliveira, A. C., & Diaconu, B. M. (2017). Analysis of a solar-assisted ejector cooling system for air conditioning. *International Journal of Low Carbon Technologies*, 12(4), 389-396.
- [31] Elakhdar, M., Landoulsia, H., Tashtoush, B., Nehdia, E., & Kairouani, L. (2019). A combined thermal system of ejector refrigeration and Organic Rankine cycles for power generation using a solar parabolic trough. *Energy*, 170, 1084-1099.
- [32] Tashtoush, B., & Algharbawi, A. R. (2019). Parametric study of a novel hybrid solar variable geometry ejector cooling with Organic Rankine cycles. *Energy Conversion and Management*, 195, 111741.
- [33] Ababneh, A. K., Jawarneh, A. M., Tlilan, H. M., & Ababneh, M. K. (2009). The effects of the secondary fluid temperature on the energy transfer in an unsteady ejector with a radial-flow diffuser. *Heat and Mass Transfer*, 46(1), 95-105. <https://doi.org/10.1007/s00231-009-0547-0>
- [34] Ani, F. N., & Kooi, K. C. (2015). The performances of a modified ejector air conditioning cycle. *International Journal of Refrigeration*, 75(11), 71-76. <https://doi.org/10.1016/j.ijrefrig.2015.07.003>
- [35] Salah, W., Taib, S., & Al-Mofleh, A. (2010). Development of multistage converter for outdoor thermal electric cooling (TEC) applications. *Jordan Journal of Mechanical and Industrial Engineering*, 4(1), 15-20.
- [36] Sharadga, H., Dawahdeh, A., & Al-Nimr, M. A. (2018). A hybrid PV/T and Kalina cycle for power generation. *International Journal of Energy Research*, 42(15), 4817-4829.
- [37] Al-Nimr, M. A., Kiwan, S., & Sharadga, H. (2018). Simulation of a novel hybrid solar photovoltaic/wind system to maintain the cell surface temperature and to generate electricity. *International Journal of Energy Research*, 8(June 2017), 985-998.
- [38] Mittelman, G., Kribus, A., & Dayan, A. (2007). Solar cooling with concentrating photovoltaic/thermal (CPVT) systems.

- Energy Conversion and Management, 48(9), 2481-2490. doi:10.1016/j.enconman.2007.04.004
- [39] Huang, B. J., Chang, J. M., Wang, C. P., & Petrenko, V. A. (1998). A 1-D analysis of ejector performance. *International Journal of Refrigeration*, 22(6), 354-364. [https://doi.org/10.1016/S0140-7007\(98\)80033-6](https://doi.org/10.1016/S0140-7007(98)80033-6)
- [40] Dubey, S., & Tiwari, G. N. (2009). Analysis of PV/T flat plate water collectors connected in series. *Solar Energy*, 83(11), 1485-1498. <https://doi.org/10.1016/j.solener.2009.08.013>
- [41] Bilgili, M. (2011). Hourly simulation, and performance of solar electric-vapor compression refrigeration system. *Solar Energy*, 85(11), 2720-2731. <https://doi.org/10.1016/j.solener.2011.08.013>
- [42] Tashtoush, B., Alshare, A., & Altarazi, S. (2017). Experimental study and statistical-based optimization of solar ejector cooling system performance with R141b as a refrigerant. In 7th International Symposium on Energy, 13th-17th August 2017.(Manchester, United Kingdom).